VNU Journal of Science: Mathematics - Physics

Journal homepage: https://js.vnu.edu.vn/MaP

Original Article

Highly Selective Separation of CO_2 and H_2 by MIL-88A Metal Organic Framework

Do Ngoc Son[1,2], Nguyen Thi Xuan Huynh[3,*], Nam Thoai[1,2], Pham Trung Kien[1,2] ,

[1]*Ho Chi Minh City University of Technology, 268 Ly Thuong Kiet, District 10, Ho Chi Minh City, Vietnam*

[2]*Vietnam National University, Ho Chi Minh City, Quarter 6, Linh Trung, Thu Duc, Ho Chi Minh City, Vietnam*

[3]*Quy Nhon University, 170 An Duong Vuong, Nguyen Van Cu, Quy Nhon, Binh Dinh, Vietnam*

Received 06 October 2020
Revised 17 November 2020; Accepted 24 December 2020

Abstract: CO_2 capture is indispensable for a cleaner environment and mitigation of global warming. The pre-combustion CO_2 capture relates to the separation of CO_2 from H_2 in the syngas mixture. Recently, metal-organic frameworks have proven to be excellent candidates for this purpose. In the current work, MIL-88A (Fe, V, Ti, Sc) were studied for the first time by using the grand canonical Monte Carlo simulations for the CO_2/H_2 mixture. The adsorption capacity of CO_2 and H_2 in the absence and presence of water medium in MIL-88A was analyzed. We found that the magnitude of the CO_2 capacity was many times higher than that of the H_2 capacity, which led to rather high CO_2/H_2 selectivity. The presence of water decreases the maximum selectivity of MIL-88A(Fe), increases that of MIL-88A(Ti and Sc), but differently influences the maximum selectivity of MIL-88A(V) for the different CO_2/H_2 mole fractions. The order of the maximum selectivity was found to be MIL-88A(Sc) > MIL-88A(Ti) > MIL-88A(V) > MIL-88A(Fe). The MIL-88A(Sc) achieved the maximum CO_2/H_2 selectivity of ~ 900 and 1300 in the absence and the presence of water medium, respectively. These values are significantly higher than those of many well-known metal-organic frameworks. The favorable adsorption sites of the CO_2/H_2 mixture in MIL-88A were also elucidated.

Keywords: Gas separation, gas capture, gas storage, metal-organic framework, simulation, hydrogen purification.

* Corresponding author.
Email address: nguyenthixuanhuynh@qnu.edu.vn

https//doi.org/ 10.25073/2588-1124/vnumap.4606

1. Introduction

The emission of CO_2 due to the escalation of the global population and the combustion of fossil fuels for energy demand has resulted in massively negative impacts on the environment and health. The concerns of global warming and air pollution have drawn special public attention to capture and reduce CO_2. Simultaneously, one has to develop new clean energy sources to replace fossil fuels. Hydrogen gas is one of the most promising candidates. The energy from hydrogen gas is environmentally friendly and non-toxic under normal conditions. Because hydrogen source is most abundant in nature as part of water, hydrocarbons, and biomass, etc., it can meet the global consumption requirement in the future crisis of energy. However, pre-combustion CO_2 capture relates to the separation of CO_2 from H_2 to afford pure H_2 in the mixture of shifted synthesis gas [1]. Therefore, the separation of CO_2 over H_2 is an important subject of sustainable development. Hydrogen gas can be used as the feeding fuel for the proton exchange membrane fuel cells, while carbon dioxide is dumped into the rock layers and under the sea or converted by green cycles into fuels such as methane, methanol, etc. [2, 3].

Many porous materials have been used to separate CO_2 from H_2 in their mixture based on the selective adsorption of the gases. Activated carbon, silica gel, carbon nanotubes, pillared clays, and zeolites have shown their potential use as adsorbents to remove CO_2 [4]. However, they suffer from low selectivity. Recently, metal-organic frameworks (MOFs) have been investigated for pressure-swing adsorption-based separation of CO_2 from H_2 [4, 5]. However, studies on this issue are still very few. The adsorption capacity of CO_2 and H_2 has been experimentally reported for MOF-177, Be-BTB, Co(BDP), Mg_2(dobdc), and Cu-BTTri [6-10]. At low pressures, the steep rise in the CO_2 adsorption isotherm of Mg_2(dobdc) among these MOFs has made Mg_2(dobdc) become the best candidate for the CO_2/H_2 separation. MOFs with localized charges in the pores such as Mg_2(dobdc) and Cu-BTTri exhibited high CO_2/H_2 selectivity while MOFs having large aromatic surfaces without significant surface charges (MOF-177, Be-BTB, Co(BDP)) displayed low CO_2/H_2 selectivity. Computational studies were also performed for the investigation of CO_2/H_2 separation. These works reported on indium-based metal-organic frameworks [11-13]. The selectivity for CO_2 over H_2 in a 15:85 CO_2/H_2 mixture at 298 K increases from 300 to 600 between 0 to 5 bar and then decreases to 450 for the increase in pressure to 30 bar [11]. The selectivity for a 50:50 CO_2/H_2 mixture was studied for HKUST-1 and MOF-5 [14]. MOF-5 shows a slow increase in the selectivity from below 10 to 30 while HKUST-1 initially decreases from 100 to 80 at 1 bar, then increases to 150 at 15 bar, and finally decreases to 100 at 50 bar.

Particularly, the MIL-88 series [15, 16], including MIL-88(A, B, C, D), have attracted our attention because (a) MIL-88 is stable in liquids, particularly with water, which can avoid collapse when exposed to a humid environment. MIL-88 series showed very high flexibility and stability. This MOF series could swell upon immersion in various liquids with reversible variations in unit cell volume from 85 to 240% depending on the nature and length of the organic spacer without breaking the bonds, and fully retains its open framework topology [17, 18]. Because of its features, the MIL-88 series has been investigated for gas adsorption and separation, drug delivery, and photo-catalyst [19-22]. (b) MIL-88 contains open metal sites, which have been shown to improve the gas uptake capacity [23-25]. (c) So far, there have been no works available for the CO_2/H_2 separation in the MIL-88 series.

Here, we focus on the investigation of MIL-88A for CO_2/H_2 separation using grand canonical Monte Carlo simulations. Through the obtained results, we gauge the capability of utilizing MIL-88A for the current concern. The scientific findings should be new and expected to be confirmed by experiments.

2. Computational Method

The grand canonical Monte Carlo simulations were executed in the μVT ensembles at the temperature of 298 K and the pressures up to 50 bar [26]. We first performed 10^5 equilibration cycles and then 2×10^5 MC steps for the translation, rotation, random insertion, and random deletion of CO_2 and H_2 in the simulation box of MIL-88A, which was repeated by $3 \times 3 \times 2$ times of the primary unit cell [27]. The MIL-88A was treated as a rigid structure, while the gas molecules were allowed to move freely in MIL-88A to reach the equilibrium state. The interaction between the gas molecules and MIL-88A were described by the Lennard-Jones and Coulomb potentials as follows:

$$U(r_{ij}) = 4\varepsilon_{ij}\left[\left(\frac{\sigma_{ij}}{r_{ij}}\right)^{12} - \left(\frac{\sigma_{ij}}{r_{ij}}\right)^{6}\right] + \frac{1}{4\pi\varepsilon_0}\frac{q_i q_j}{r_{ij}}. \quad (1)$$

Here, r_{ij} is the distance between two unlike atoms i and j. The dielectric constant of vacuum space is ε_0. The partial charge of the i^{th} atom is q_i, which was previously obtained by the DFT-based DDEC net atomic charge method [27-29]. The Ewald summation was applied to treat the Coulomb interaction with the cut-off radius of 12 Å. The Lennard-Jones potential well-depth and diameter ε_{ij} and σ_{ij} were determined using the Lorentz-Berthelot mixing rule for a pair of unlike atoms,

$$\varepsilon_{ij} = \sqrt{\varepsilon_i \varepsilon_j}, \quad \sigma_{ij} = \frac{1}{2}(\sigma_i + \sigma_j). \quad (2)$$

In which, ε_i and σ_i were taken from the generic force fields for the H, C, O, Sc, Ti, V, and Fe atoms of MIL-88A [26], (see Table 1). The cut-off radius for the Lennard-Jones interaction was set at 14 Å. The hydrogen molecule was modeled by the single site H_{com} at the center of mass of the hydrogen molecule using the TraPPE force field [30], and the CO_2 molecule was modeled as a rigid site using the EPM2 force field [31].

Table 1. The force field parameters for MIL-88A, H_2, and CO_2.

Atoms	ε/k_B (K)	σ (Å)	Partial charge (e)
Sc	9.56	2.94	2.09
Ti	8.55	2.83	1.90
V	8.05	2.80	1.76
Fe	6.54	2.59	1.22
H	7.65	2.85	0.118
C in COO- group	47.86	3.47	0.734
C in -C_2H_2- group			-0.178
O in COO- group	48.16	3.03	-0.570
μ_3-O (at center of trimer)			-0.875
H_{com} (H_2) [30]	36.70	2.96	-0.94
C (in CO_2) [31]	27.00	2.80	0.70
O (in CO_2) [31]	79.00	3.05	-0.35

The selectivity of CO_2 relative to H_2 is calculated by [4]:

$$S = \frac{n_A N_B}{N_A n_B}. \quad (3)$$

Where, n_A and n_B are the molar fractions of CO_2 and H_2 in the adsorbed state of their mixture and N_A and N_B are those in the bulk state, respectively.

3. Results and Discussion

3.1. Adsorption Isotherms of CO_2/H_2 Mixture

The geometry structure of MIL-88A with different transition metals Fe, V, Ti, and Sc was optimized based on the DFT calculations in the previous publication [27]. With the optimized structure, we built the simulation box as mentioned in the computational method section. We calculated the adsorption isotherm for the mixture of CO_2/H_2, which is often considered for the understanding of the gas adsorption ability of porous materials. In the literature, most of the publications studied the isotherm for each gas separately. However, for the study of the gas separation, we have to simulate and analyze the adsorption isotherm for the gas mixture. In the pre-combustion, the syngas includes the gas compositions of about 36% CO_2, 62% H_2, less than 1% H_2O [32]. Therefore, we will also elucidate the effects of water medium on the adsorption isotherm and selectivity of CO_2 from H_2 at room temperature by considering two cases that are in the presence and absence of H_2O. Taking into account the influences of the other compositions of the syngas is out of the scope.

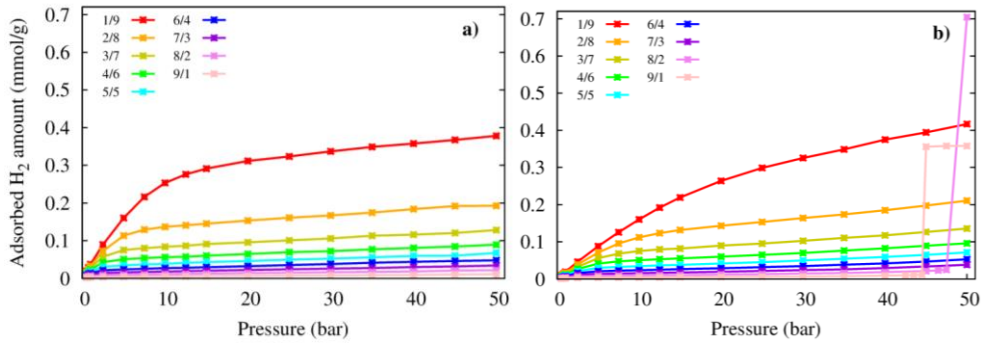

Figure 1. The H_2 adsorption capacity of MIL-88A(Fe) for the different ratios of CO_2/H_2 mole fractions at 298 K without H_2O (a) and with H_2O (b).

Figure 1 shows the adsorption isotherms of hydrogen gas in MIL-88A(Fe) in the absence and the presence of H_2O. Figure 1a exhibits that the magnitude of the isotherm increases as the mole ratios of CO_2/H_2 decrease. At the mole ratios of $CO_2/H_2 \geq 5/5$, the isotherms are very small and almost flat with the increase in pressure. At the ratios < 5/5, the magnitude of isotherms is more significant, and each curve increases more rapidly with the pressure. Compared to the results obtained for the single gas component of H_2 in MIL-88A [27], the isotherms for H_2 in the CO_2/H_2 mixture (this work) are more abruptly varied with the pressure than the monotonic behavior of the single gas adsorption isotherm [27]. In the presence of water medium, Figure 1b exhibits that besides the behavior that is similar to the case of without H_2O, at the high mole ratios of CO_2/H_2, i.e., 8/2 and 9/1, the sudden increase in the H_2 isotherm implies that the hydrogen adsorption capacity is sensitive to the water medium. However, for the other CO_2/H_2 mole ratios, the water medium generates the ignorable enhancement of the H_2 adsorption isotherm compared to the case without water.

The CO_2 adsorption capacity gradually increases with the increase of the pressure at the low CO_2/H_2 ratio, i.e., 1/9, and rapidly at the higher CO_2/H_2 mole ratios at the pressures below 10 bar (see Figure 2a). The saturation of each isotherm curve achieves at the pressure of about 50 bar. The higher the CO_2/H_2 mole ratio, the higher the magnitude of the isotherm is. This tendency is opposite to that of H_2 adsorption. The absolute value of the CO_2 isotherm is also many times higher than that of H_2. Figure 2b shows that each curve of CO_2 isotherms in the presence of H_2O has similar behavior to that of the case without

H_2O, but with a lower magnitude. Especially at high mole ratios such as 8/2 and 9/1, a little increase in the isotherm arises at the pressure greater than 45 bar. From the above analysis, we can see that the presence of water does not only increase the CO_2 adsorption isotherm but also the H_2 isotherm at pressures around 45 bar for high mole ratios of CO_2/H_2.

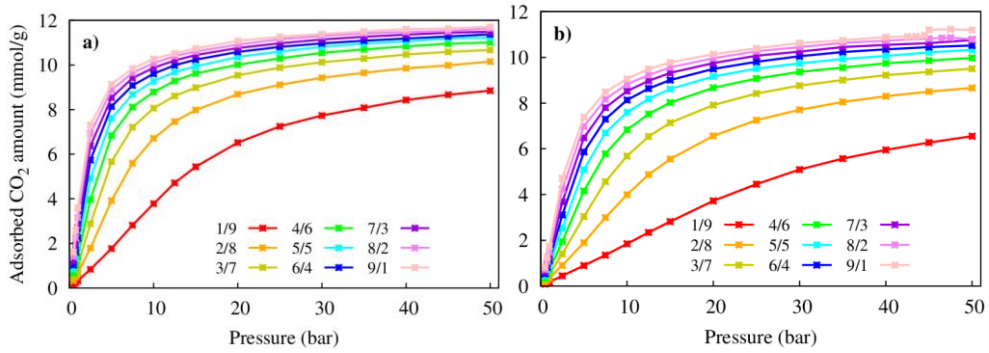

Figure 2. The CO_2 adsorption capacity of MIL-88A(Fe) for the different CO_2/H_2 mole fractions at 298 K without H_2O (a) and with H_2O (b).

3.2. Adsorption Selectivity of CO_2 Relative to H_2

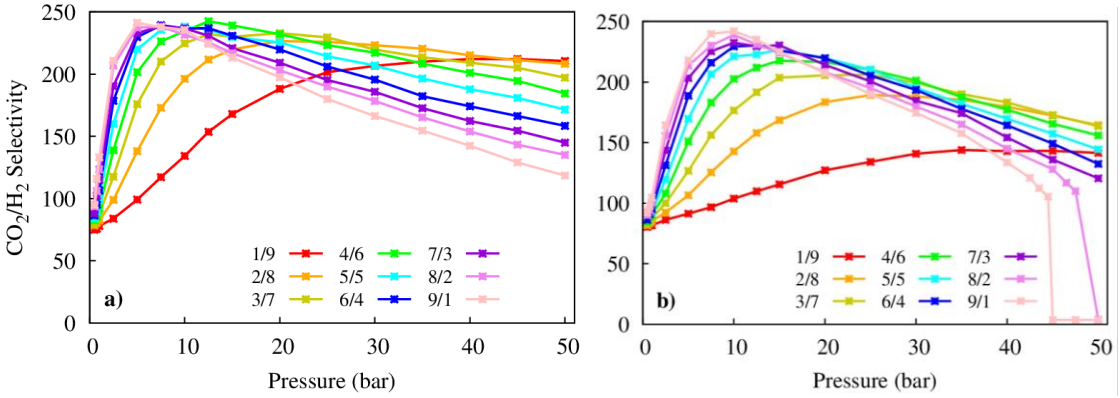

Figure 3. The CO_2/H_2 selectivity capacity of MIL-88A(Fe) for the different CO_2/H_2 mole fractions at 298 K without H_2O (a) and with H_2O (b).

From the obtained adsorption isotherms of H_2 and CO_2 as shown in Figures 1 and 2, we calculated the CO_2/H_2 selectivity following the equation (3). We found that each curve of the selectivity had a maximum (see Figure 3). The higher the CO_2/H_2 mole ratio, the higher the maximum of the selectivity was obtained. Also, the position of the maximum shifts to the lower pressure for the higher CO_2/H_2 mole ratio. Figure 3b shows that, for each ratio of CO_2/H_2, the CO_2/H_2 selectivity in the presence of water is much lower than that compared to the case of without water. For the CO_2/H_2 ratios of 8/2 and 9/1, the selectivity suddenly drops at around 45 to 50 bar, which also correlates to the sudden changes in the adsorption isotherms of H_2 and CO_2 as discussed above.

The substitution of metal sites with different transition metals is a viable strategy to improve the adsorption capacity of gases [23]. Therefore, we also expect that the metal substitution can enhance the selectivity of the CO_2 over H_2. Here, we consider the replacement of the Fe sites of MIL-88A by Sc, Ti,

and V and investigate the selectivity of CO_2 over H_2 in their mixture with the presence and absence of H_2O. The detailed study was performed for the CO_2/H_2 mole fractions of 1/9, 5/5, and 9/1 and presented in Figures 4a, b, and c, respectively. For the mole fraction of 1/9, Figure 4a shows that the selectivity of CO_2 over H_2 for MIL-88A(Fe and V) increases to a maximum value then decreases with the increase in the pressure, while the selectivity for MIL-88A(Sc and Ti) decreases monotonically. The presence of water reduces the selectivity for MIL-88A(Fe and V) at high pressures, while it enhances that for MIL-88A(Sc and Ti) at low pressures. From Figures 4b and c, we find that the selectivity in the absence of water shows similar behavior for both 5/5 and 9/1 ratios of mole fraction. However, in the presence of water, the behavior for the 9/1 mole ratio is different compared to that for the 5/5 ratio, i.e., the selectivity suddenly drops at about 45 bar for the 9/1 ratio, which relates to the sudden change of the isotherms of CO_2 and H_2 as already pointed out in the above discussion.

Table 2. The maximum selectivity of CO_2 over H_2 in the gas mixture in MIL-88A at 298 K.

CO_2/H_2 mole fraction		**Absence of H_2O**	**Presence of H_2O**
MIL-88A(Fe)	1:9	212.15 (45 bar)	143.18 (45 bar)
	2:8	226.53 (20 bar)	189.24 (25 bar)
	3:7	232.89 (20 bar)	206.06 (25 bar)
	4:6	242.48 (12.5 bar)	217.65 (15 bar)
	5:5	238.14 (10 bar)	226.72 (15 bar)
	6:4	239.34 (7.5 bar)	230.27 (12.5 bar)
	7:3	238.60 (7.5 bar)	232.55 (10 bar)
	8:2	238.09 (7.5 bar)	238.97 (10 bar)
	9:1	243.75 (5.0 bar)	242.01 (10 bar)
MIL-88A(V)	1:9	334.50 (20 bar)	292.19 (25 bar)
	4:6	342.74 (7.5 bar)	345.04 (10 bar)
	5:5	346.61 (5.0 bar)	346.74 (7.5 bar)
	9:1	344.52 (2.5 bar)	360.46 (5.0 bar)
MIL-88A(Ti)	1:9	435.80 (1 bar)	492.95 (1 bar)
	4:6	376.93 (1 bar)	423.24 (1 bar)
	5:5	382.25 (1 bar)	421.52 (1 bar)
	9:1	385.38 (1 bar)	410.73 (1 bar)
MIL-88A(Sc)	1:9	924.43 (1 bar)	1382.71 (1 bar)
	4:6	579.57 (1 bar)	743.13 (1 bar)
	5:5	546.36 (1 bar)	693.29 (1 bar)
	9:1	490.79 (1 bar)	610.29 (1 bar)
***soc*-MOF** [11]		600 (3 bar)	
Cu-BTC [14]		< 150 (0 – 60 bar)	
MOF-5 [14]		< 50 (0 – 60 bar)	
IRMOF-*n* (*n* = 9 ~ 14) [33]		< 120 (0 – 20 bar)	

Table 2 lists the maximum selectivity of CO_2 over H_2 in the presence and the absence of H_2O in MIL-88A with different transition metals. We find that the replacement of Fe by V, Ti, and Sc can enhance the maximum value. Also, the presence of water could drastically improve the maximum value of selectivity for V, Ti, and Sc, where Sc was found to be the best candidate for the separation of CO_2 and H_2. The selectivity was also found to be much higher for MIL-88A than the other metal-organic frameworks such as Cu-BTC, MOF-5 [14], IRMOF-*n* (n = 9 ~ 14) [33], and comparable to soc-MOF

[11]. For further understanding of the role of water, Figure 5 reveals the adsorption capacity of H_2O in MIL-88A with different metals, which shows the same behavior for different CO_2/H_2 mole fractions. We see that the H_2O capacity exhibits a sudden increase at low pressures below 2 bar and reaches a saturation value of about 0.11 mmol/g after that. Its saturation value is almost the same for different metals and different mole fractions of CO_2/H_2. The water capacity does not increase at around 45 bar as the H_2 and CO_2 adsorption capacity does.

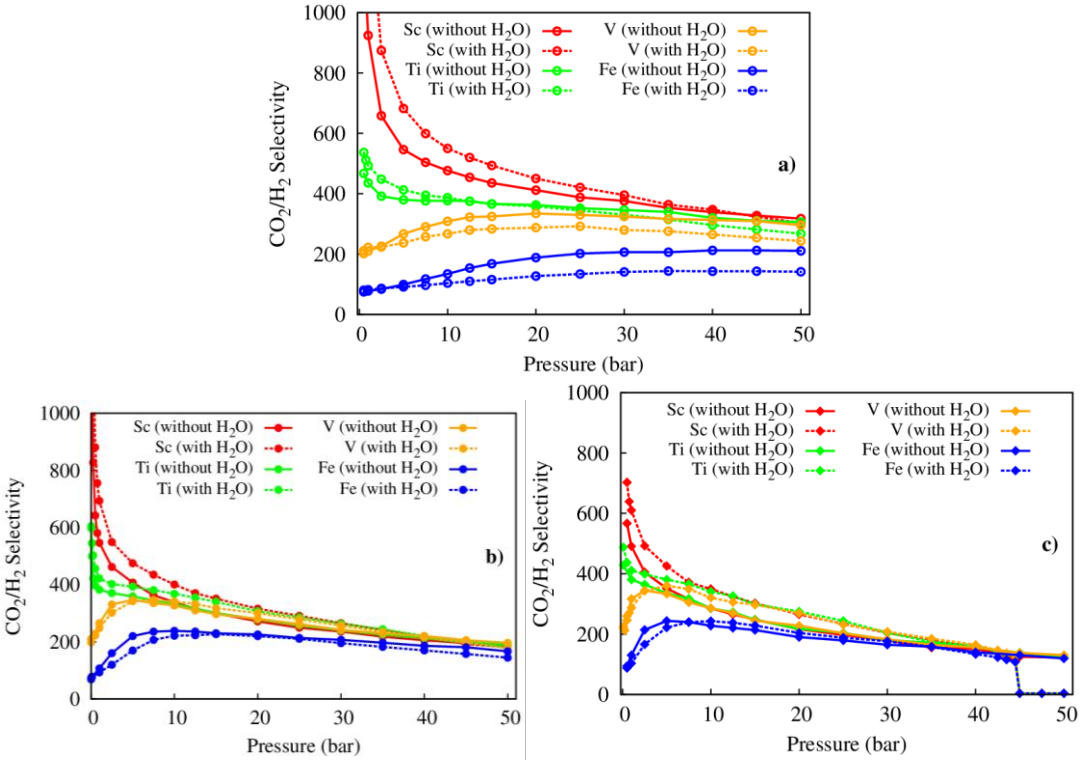

Figure 4. The CO_2/H_2 selectivity of MIL-88A(Sc, Ti, V, Fe) for the CO_2/H_2 mole fraction of 1/9 (a), 5/5 (b), and 9/1 (c).

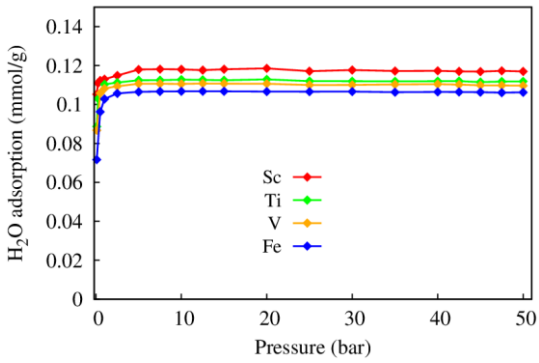

Figure 5. The adsorption capacity of H_2O in MIL-88A (Sc, Ti, V, Fe) with the presence of the CO_2/H_2 mixture for the 9/1 mole fraction at 298 K. For the other mole fractions, the behavior of the H_2O adsorption isotherm was found to be similar to that of 9/1.

To elucidate the contributions of Coulomb and Lennard-Jones interactions to the CO_2/H_2 selectivity, we separately included the Lennard-Jones interaction in the GCMC simulations for the CO_2/H_2 gas mixture, while excluding the Coulomb. We found that the selectivity, as presented in Figure 6, showed the small magnitude only below 60. The dispersive interaction varies the selectivity in the range of only 30 units in the parabolic manner with the maximum value reaching 20 bar. These values are low compared to those for the full inclusion of both interactions. By comparing Figure 6 with Figure 4b, we deduce that the main contribution to the CO_2/H_2 selectivity should come from the Coulomb interaction.

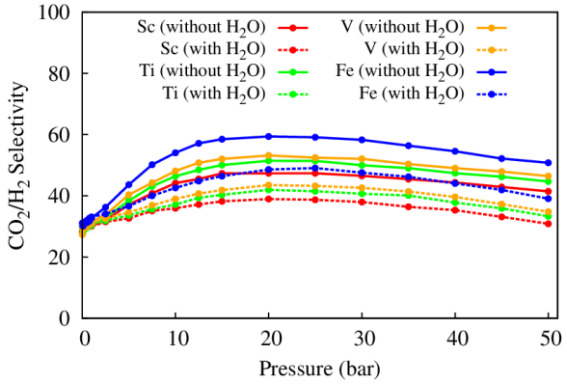

Figure 6. The CO_2/H_2 selectivity of MIL-88A (Sc, Ti, V, and Fe) for the CO_2/H_2 mole fraction of 5/5 with the inclusion of only the dispersive Lennard-Jones interaction at 298 K.

3.3. Adsorption Mechanism of CO_2 and H_2 in MIL-88A

We can understand the adsorption mechanism and preferential binding sites of CO_2 and H_2 by considering the snapshots of the gas mixture in the MIL-88A structure with the variation of pressure. We already saw in Figure 4 that the selectivity behavior for Fe and Sc was similar to that for V and Ti, respectively. Furthermore, while analyzing the obtained results, we also found the adsorption mechanism and preferential binding sites of MIL-88A(Fe and Sc) systems were similar to that of MIL-88A(V and Ti) in that order. Therefore, in this section, we focus our discussion on MIL-88A(Fe and Sc) as two representatives. Figure 7 shows the snapshots of MIL-88A(Fe) with the viewpoints of the large and small pores at 5, 10, 15, and 50 bar. The adsorption of the gases was found most favorable at the ligand sites. The increase in pressure enhances the concentration of CO_2 at the ligand sites and then the metal sites before filling the free space of the pores. In the simulation cell, the number of H_2 molecules is less than that of CO_2 molecules. At the low pressure, i.e., 5 bar, the probability of finding H_2 in the simulation cell is not high enough to display in the snapshot. However, at higher pressures, we can see the occurrence of the H_2 molecules, which is presented by the three-point model with H_{com} in green color.

To avoid a large number of figures, we don't systematically present the snapshots of MIL-88A(Sc) for different pressures. Figures 8a and c exhibit that, in the absence of H_2O, the preferential binding sites of the CO_2 molecules are the metal and ligand sites for MIL-88A(Sc). It is unclear which site is more dominated. In the presence of H_2O, it is more evident in Figures 8b and d that the Sc sites become more dominated for CO_2 with a higher density of CO_2 at the Sc sites and hence improve the selectivity of CO_2 over H_2, as shown in Figure 4. Therefore, the effect of H_2O is to enhance the population of CO_2 at the metal sites of MIL-88A(Sc). Also, by comparing Figures 8b and d with Figures 7b and g, we observed that the density of the CO_2 molecules in MIL-88A(Sc) was significantly higher than that in MIL-88A(Fe) at the same pressure.

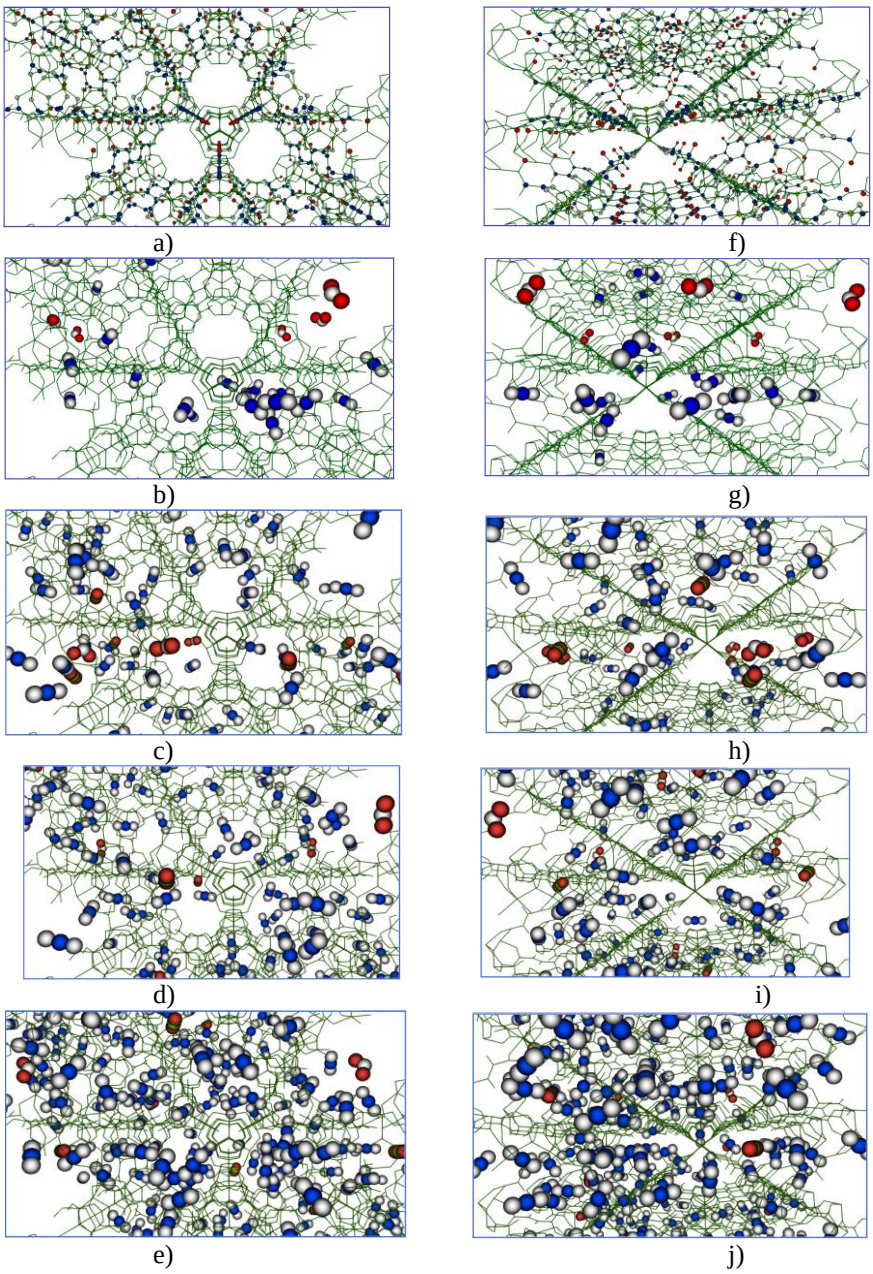

Figure 7. The snapshots of the CO_2/H_2 mixture in the presence of H_2O in MIL-88A(Fe) at the CO_2/H_2 mole fraction of 1/9. The left and right panels are the different views of the structure of MIL-88A(Fe) with the large and narrow pores, respectively. Figures a) and f) are the structure of MIL-88A(Fe) without the adsorbates: ligand site with red and blue dots, and metal site with yellow spots. The second to the last row are the snapshots for the pressures of 5, 10, 15, and 50 bar, respectively. Here, C (blue), O (gray), H (red), Fe (yellow), H_{com} (green). The hydrogen molecule is presented by the three-point model with H_{com} to increase the visibility. Since the distribution of the gas molecules in the absence and presence of H_2O is similar for MIL-88A(Fe), we presented here only for the presence of H_2O.

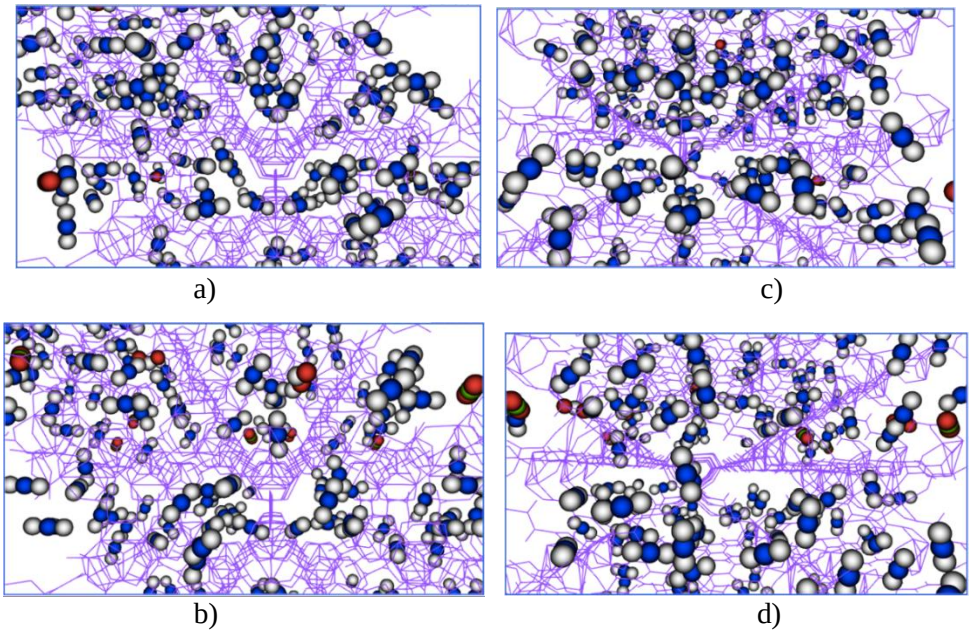

Figure 8. The upper and bottom panels are the snapshots of MIL-88A(Sc) with the adsorbates in the absence and presence of H_2O at 5 bar, respectively. Left (the large pore) and right (the narrow pore).

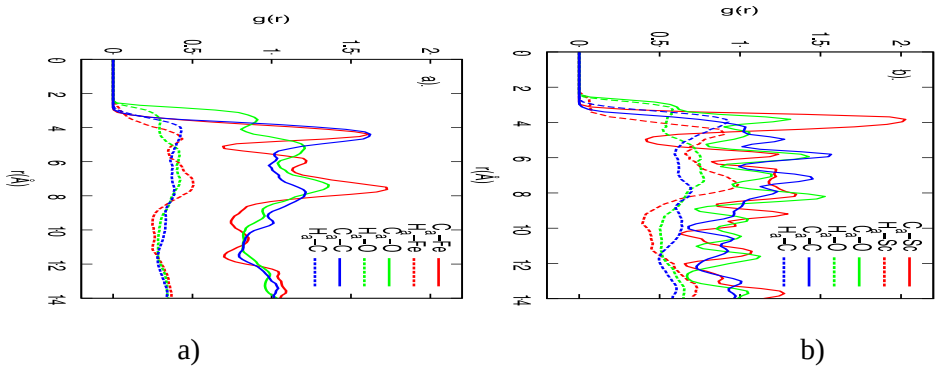

Figure 9. Radial distribution functions at 5 bar for the CO_2/H_2 mixture in the presence of H_2O in (a) MIL-88A(Fe) and (b) MIL-88A(Sc),where, C_a and H_a denote the carbon atom of CO_2 and H_{com} of H_2, respectively.

It is rather difficult to understand the preferential binding sites of H_2 based on the snapshots in Figures 7 and 8. Radial distribution functions, presented in Figure 9, are more transparent. We can find the distribution of CO_2 and H_2 around the reference atoms, i.e., Fe, Sc, O, and C of the metal-organic framework as a function of the distance from C of CO_2 (C_a) and H_{com} of H_2 (H_a) to the reference atoms. The first peak shows the density of the gases at the nearest distance. Figure 9 exhibits that the first peak of C_a-C is slightly higher than C_a-Fe, implying that the ligand site is more favorable than the metal site for CO_2. Also, CO_2 mainly distributes around the ligand and metal sites rather than around the oxygen atoms of MIL-88A(Fe). The behavior of the H_2 distribution in MIL-88A(Fe) is similar to that of CO_2 but with a significantly smaller magnitude. In MIL-88A(Sc), the O and Sc atoms are the nearest neighbors. Therefore, from Figure 9b, we find that the metal nodes are the most favorable for CO_2 adsorption. Furthermore, the multi-peaks nature in the radial distribution functions of CO_2 indicates that

CO_2 also scatters at many different sites besides the preferential (metal) sites. However, the H_2 molecules prefer the ligand sites more than the metal sites in MIL-88A(Sc), which is similar to its behavior in MIL-88A(Fe). The strong adsorption at the metal sites and the scattering distribution of CO_2 in MIL-88A(Sc) perhaps should be the reasons for the improved selectivity of the MIL-88A(Sc) metal-organic framework.

We also make efforts to clarify the abnormal behavior of the adsorption isotherms of H_2 and CO_2 at high pressures around 50 bar for the high mole fractions of CO_2/H_2 such as 8/2 and 9/1; however, we could not justify whether it relates to the sensitivity of the selected force field parameters or physical meanings. This open question is reserved forfuture work.

4. Conclusion

In this paper, we have assessed the capability of MIL-88A(Fe, V, Ti, and Sc) for the separation of CO_2 over H_2 in their mixture with the absence and presence of the water medium. By performing the GCMC simulations with force field parameters partly built from the point charges obtained from the density functional theory calculations, we studied the adsorption capacity of CO_2, H_2, and H_2O, and also the CO_2/H_2 selectivity. We have found that MIL-88A is an excellent candidate for the CO_2/H_2 separation. Also, the replacement of Fe by V, Ti, and Sc was found to improve the separation performance significantly,in which, Sc was found to be the best for a superior CO_2/H_2 selectivity. The H_2O medium enhanced the selectivity for MIL-88A(Sc, Ti) due to the increase in the CO_2 density around the metal sites.

Acknowledgments

This research was funded by the National Foundation for Science and Technology Development (NAFOSTED) under Grant 103.01-2017.04. We acknowledge the usage of computer time granted by the High-Performance Computing Lab, Faculty of Computer Science and Engineering, University of Technology, Vietnam National University, Ho Chi Minh City.

References

[1] K. Sumida, D. L. Logow, J. A. Mason, T. M. McDonald, E. D. Bloch, Z. R. Herm, T. H. Bae, J. R. Long, Carbon Dioxide Capture in Metal-Organic Frameworks, Chem. Rev., Vol. 112, No. 2, 2012, pp. 724-781, https://doi.org/10.1021/cr2003272.

[2] W. Li, H. Wang, X. Jiang, J. Zhu, Z. Liu, X. Guo, C. Song, A Short Review of Recent Advances in CO_2 Hydrogenation to Hydrocarbons over Heterogeneous Catalysts, RSC Adv., Vol. 8, 2018, pp. 7651-7669, https://doi.org/10.1039/C7RA13546G.

[3] J. Artz, T. E. Müller, K. Thenert, J. Kleinekorte, R. Meys, A. Sternberg, A. Bardow, W. Leitner, Sustainable Conversion of Carbon Dioxide: An Integrated Review of Catalysis and Life Cycle Assessment, Chem. Rev., Vol. 118, No. 2, 2018, pp. 434-504, https://doi.org/10.1021/acs.chemrev.7b00435.

[4] J. R. Li, R. J. Kuppler, H. C. Zhou, Selective Gas Adsorption and Separation in Metal–Organic Frameworks, Chem. Soc. Rev., Vol. 38, 2009, pp. 1477-1504, https://doi.org/10.1039/B802426J.

[5] T. T. T. Huong, P. N. Thanh, N. T. X. Huynh, D. N. Son, Metal – Organic Frameworks: State-of-the-art Material for Gas Capture and Storage, VNU J. Sci.: Math. Phys., Vol. 32, No. 1, 2016, pp. 67-85, https://js.vnu.edu.vn/MaP/article/view/428.

[6] K. Sumida, M. R. Hill, S. Horike, A. Dailly, J. R. Long, Synthesis and Hydrogen Storage Properties of $Be_{12}(OH)_{12}$(1,3,5-benzenetribenzoate)$_4$, J. Am. Chem. Soc., Vol. 131, No. 42, 2009, pp. 15120-15121, https://doi.org/10.1021/ja9072707.

[7] H. K. Chae, D. Y. S. Perez, J. Kim, Y. B. Go, M. Eddaoudi, A. J. Matzger, M. O'Keeffe, O. M. Yaghi, A Route to High Surface Area, Porosity and Inclusion of Large Molecules in Crystals, Nature, Vol. 427, 2004, pp. 523-527, https://doi.org/10.1038/nature02311.

[8] H. J. Choi, M. Dinca, J. R. Long, Broadly Hysteretic H_2 Adsorption in The Microporous Metal-Organic Framework Co(1,4-benzenedipyrazolate), J. Am. Chem. Soc., Vol. 130, No. 25, 2008, pp. 7848-7850, https://doi.org/10.1021/ja8024092.

[9] S. R. Caskey, A. G. W. Foy, A. Matzger, Dramatic Tuning of Carbon Dioxide Uptake via Metal Substitution in A Coordination Polymer with Cylindrical Pores, J. Am. Chem. Soc., Vol. 130, No. 33, 2008, pp. 10870-10871, https://doi.org/10.1021/ja8036096.

[10] A. Demessence, D. M. D.'Alessandro, M. L. Foo, J. R. Long, Strong CO_2 Binding in A Water-stable, Triazolate-bridged Metal-Organic Framework Functionalized with Ethylenediamine, J. Am. Chem. Soc., Vol. 131, No. 25, 2009, pp. 8784-8786, https://doi.org/10.1021/ja903411w.

[11] J. Jiang, Charged *soc* Metal-Organic Framework for High-efficacy H_2 Adsorption and Syngas Purification: Atomistic Simulation Study, AIChE J., Vol. 55, No. 9, 2009, pp. 2422-2432, https://doi.org/10.1002/aic.11865.

[12] R. Babarao, J. W. Jiang, Cation Characterization and CO_2 Capture in Li^+-exchanged Metal−Organic Frameworks: From First-principles Modeling to Molecular Simulation, Ind. Eng. Chem. Res., Vol. 50, No. 1, 2011, pp. 62-68, https://doi.org/10.1021/ie100214a.

[13] R. Babarao, J. W. Jiang, Unprecedentedly High Selective Adsorption of Gas Mixtures in *rho* Zeolite-like Metal-Organic Framework: A Molecular Simulation Study, J. Am. Chem. Soc., Vol. 131, No. 32, 2009, pp. 11417-11425, https://doi.org/10.1021/ja901061j.

[14] Q. Yang, C. Zhong, Molecular Simulation of Carbon Dioxide/Methane/Hydrogen Mixture Adsorption in Metal-Organic Frameworks, J. Phys. Chem. B, Vol. 110, No. 36, 2006, pp, 17776-17783, https://doi.org/10.1021/jp062723w.

[15] S. Surblé, C. Serre, C. M. Draznieks, F. Millange, G. Férey, A New Isoreticular Class of Metal-Organic-frameworks with the MIL-88 topology, Chem. Commun., 2006, pp. 284-286, https://doi.org/10.1039/B512169H.

[16] C. M. Draznieks, C. Serre, S. Surblé, N. Audebrand, G. Férey, Very Large Swelling in Hybrid Frameworks: A Combined Computational and Powder Diffraction Study, J. Am. Chem. Soc., Vol. 127, No. 46, 2005, pp. 16273-16277, https://doi.org/10.1021/ja054900x.

[17] P. Horcajada, F. Salles, S. Wuttke, T. Devic, D. Heurtaux, G. Maurin, A. Vimont, M. Daturi, O. David, E. Magnier, N. Stock, Y. Filinchuk, D. Popov, C. Riekel, G. Férey, C. Serre, How Linker's Modification Controls Swelling Properties of Highly Flexible Iron(III) Dicarboxylates MIL-88, J. Am. Chem. Soc., Vol. 133, No. 44, 2011, pp. 17839-17847, https://doi.org/10.1021/ja206936e.

[18] N. A. Ramsahye, T. K. Trung, L. Scott, F. Nouar, T. Devic, P. Horcajada, E. Magnier, O. David, C. Serre, P. Trens, Impact of the Flexible Character of MIL-88 Iron(III) Dicarboxylates on the Adsorption of n-Alkanes, Chem. Mater., Vol. 25, No, 3, 2013, pp. 479-488, https://doi.org/10.1021/cm303830b.

[19] M. Ma, H. Noei, B Mienert, J. Niesel, E. Bill, M. Muhler, R. A. Fischer, Y. Wang, U. Schatzschneider, N. M. Nolte, Iron Metal-Organic Frameworks MIL-88B and NH_2-MIL-88B for The Loading and Delivery of The Gasotransmitter Carbon Monoxide, Chem. Eur. J., Vol. 19, No. 21, 2013, pp. 6785-6790, https://doi.org/10.1002/chem.201201743.

[20] Y. Xiao, X. Guo, H. Huang, Q. Yang, A. Huang, C. Zhong, Synthesis of MIL-88B(Fe)/Matrimid Mixed-matrix Membranes with High Hydrogen Permselectivity, RSC Adv., Vol. 5, 2015, pp. 7253-7259, https://doi.org/10.1039/C4RA13727B.

[21] A. C. McKinlay, J. F. Eubank, S. Wuttke, B. Xiao, P. S. Wheatley, P. Bazin, J. C. Lavalley, M. Daturi, A. Vimont, G. De Weireld, P. Horcajada, C. Serre, R. E. Morris, Nitric Oxide Adsorption and Delivery in Flexible MIL-88(Fe) Metal-Organic Frameworks, Chem. Mater., Vol. 25, No. 9, 2013, pp. 1592-1599, https://doi.org/10.1021/cm304037x.

[22] W. T. Xu, L. Ma, F. Ke, F. M. Peng, G. S. Xu, Y. H. Shen, J. F. Zhu, L. G. Qiu, Y. P. Yuan, Metal-Organic Frameworks MIL-88A Hexagonal Microrods as A New Photocatalyst for Efficient Decolorization of Methylene Blue Dye, Dalton Trans., Vol. 43, No. 9, 2014, pp. 3792-3798, https://doi.org/10.1039/C3DT52574K.

[23] J. L. C. Rowsell, O. M. Yaghi, Strategies for Hydrogen Storage in Metal-Organic Frameworks, Angew. Chem. Int. Ed., Vol. 44, No. 30, 2005, pp. 4670-4679, https://doi.org/10.1002/anie.200462786.

[24] M. P. Suh, H. J. Park, T. K. Prasad, D. W. Lim, Hydrogen Storage in Metal-Organic Frameworks, Chem. Rev., Vol. 112, No. 2, 2012, pp. 782-835, https://doi.org/10.1021/cr200274s.

[25] L. J. Murray, M. Dincă, J. R. Long, Hydrogen Storage in Metal-Organic Frameworks, Chem. Soc. Rev., Vol. 38, 2009, pp. 1294-1314, https://doi.org/10.1039/B802256A.

[26] D. Dubbeldam, S. Calero, D. E. Ellis, and R. Q. Snurr, RASPA: Molecular Simulation Software for Adsorption and Diffusion in Flexible Nanoporous Materials, Mol. Simul., Vol. 42, No. 2, 2016, pp. 81-101, https://doi.org/10.1080/08927022.2015.1010082.

[27] N. T. X. Huynh, V. Chihaia, D. N. Son, Enhancing Hydrogen Storage by Metal Substitution in MIL-88A Metal-Organic Framework, Adsorption, Vol. 26, 2020, pp. 509-519, https://doi.org/10.1007/s10450-020-00213-8.

[28] N. T. X. Huynh, V. Chihaia, D. N. Son, Hydrogen Storage in MIL-88 Series, J. Mater Sci., Vol. 54, 2019, pp. 3994-4010, https://doi.org/10.1007/s10853-018-3140-4.

[29] T. A. Manz, D. S. Sholl, Improved Atoms-in-Molecule Charge Partitioning Functional for Simultaneously Reproducing The Electrostatic Potential and Chemical States in Periodic and Nonperiodic Materials, J. Chem. Theory Comput., Vol. 8, No. 8, 2012, pp. 2844-2867, https://doi.org/10.1021/ct3002199.

[30] D. Levesque, A. Gicquel, F. L. Darkrim, S. B. Kayiran, Monte Carlo Simulations of Hydrogen Storage in Carbon Nanotubes, J. Phys. Condens. Matter, Vol. 14, No. 40, 2002, pp. 9285-9293, https://doi.org/10.1088/0953-8984/14/40/318.

[31] J. G. Harris, K. H. Yungt, Carbon Dioxide's Liquid-Vapor Coexistence Curve and Critical Properties as Predicted by A Simple Molecular Model, J. Phys. Chem., Vol. 99, No. 31, 1995, pp. 12021-12024, https://doi.org/10.1021/j100031a034.

[32] D. M. D. Alessandro, B. Smit, J. R. Long, Carbon Dioxide Capture: Prospects for New Materials, Angew. Chem. Int. Ed., Vol. 49, No. 35, 2010, pp. 6058-6082, https://doi.org/10.1002/anie.201000431.

[33] Y. Qingyuan, X. U. Qing, L. I. U. Bei, Z. Chongli, Molecular Simulation of CO_2/H_2 Mixture Separation in Metal-Organic Frameworks: Effect of Catenation and Electrostatic Interactions, Chinese J. Chem. Eng., Vol. 17, No. 5, 2009, pp. 781-790, https://doi.org/10.1016/S1004-9541(08)60277-3.